ARTICLE

Phosphoproteomic approach for agonist-specific signaling in mouse brains: mTOR pathway is involved in κ opioid aversion

Jeffrey J. Liu [1], Yi-Ting Chiu[2], Kelly M. DiMattio[2], Chongguang Chen[2], Peng Huang[2], Taylor A. Gentile[2], John W. Muschamp[2], Alan Cowan[2], Matthias Mann[1] and Lee-Yuan Liu-Chen[2]

Kappa opioid receptor (KOR) agonists produce analgesic and anti-pruritic effects, but their clinical application was limited by dysphoria and hallucinations. Nalfurafine, a clinically used KOR agonist, does not cause dysphoria or hallucinations at therapeutic doses in humans. We found that in CD-1 mice nalfurafine produced analgesic and anti-scratch effects dose-dependently, like the prototypic KOR agonist U50,488H. In contrast, unlike U50,488H, nalfurafine caused no aversion, anhedonia, or sedation or and a low level of motor incoordination at the effective analgesia and anti-scratch doses. Thus, we established a mouse model that recapitulated important aspects of the clinical observations. We then employed a phosphoproteomics approach to investigate mechanisms underlying differential KOR-mediated effects. A large-scale mass spectrometry (MS)-based analysis on brains revealed that nalfurafine perturbed phosphoproteomes differently from U50,488H in a brain-region specific manner after 30-min treatment. In particular, U50,488H and nalfurafine imparted phosphorylation changes to proteins found in different cellular components or signaling pathways in different brain regions. Notably, we observed that U50,488H, but not nalfurafine, activated the mammalian target of rapamycin (mTOR) pathway in the striatum and cortex. Inhibition of the mTOR pathway by rapamycin abolished U50,488H-induced aversion, without affecting analgesic, anti-scratch, and sedative effects and motor incoordination. The results indicate that the mTOR pathway is involved in KOR agonist-induced aversion. This is the first demonstration that phosphoproteomics can be applied to agonist-specific signaling of G protein-coupled receptors (GPCRs) in mouse brains to unravel pharmacologically important pathways. Furthermore, this is one of the first two reports that the mTOR pathway mediates aversion caused by KOR activation.

INTRODUCTION

KOR is expressed mainly in the nervous systems in mammals. Activation of the KOR produces many effects, such as analgesia, antipruritic effect, water diuresis, dysphoria/aversion, sedation, motor incoordination, and psychotomimetic effects, including hallucinations [1–6]. Selective KOR agonists are effective analgesics, but without respiratory depression and abuse potential associated with mu opioid receptor (MOR)-preferring analgesics such as morphine and fentanyl [7]. Selective KOR agonists are also promising antipruritic agents and water diuretics. However, clinical applications of KOR agonists are limited by dysphoria and psychotomimetic effects in humans [4, 8], except for nalfurafine in most patients. Salvinorin A, the active component of the hallucinogenic plant *Salvia divinorum*, was identified to be a selective KOR agonist [5].

Nalfurafine has been used in Japan for treatment of pruritus in hemodialysis patients [9–12]. Notably, at the therapeutic doses, dysphoria was not reported as an adverse drug reaction and hallucinations occurred at a low rate (0.25%) [9–11], making it a valuable tool compound for study of KOR-mediated side effects. Specifically, comparison of treatment of animals with nalfurafine and classic aversive KOR-specific agonists can yield biochemical

insights to this important clinical observation. Two selective KOR agonists were used for comparison. U50,488H is the prototypic KOR-selective agonist [13]. Methoxymethyl salvinorin B (MOM-SalB) [14] is an analog of salvinorin A with a longer duration of action (chemical structures in Fig. S1).

Our understanding of KOR signal transduction is largely derived from in vitro studies. As a G protein-coupled receptor (GPCR), KOR activates G protein-dependent and arrestin-dependent signaling in parallel. Some GPCR agonists preferentially activate G protein-dependent or arrestin-dependent signaling, which is referred to as "functional selectivity" or "biased signaling" [15, 16]. The concept of functional selectivity predicts that biased ligands impart different behavioral responses, raising the hope of reduced side effects without impacting the therapeutic efficacy. Conditioned place aversion (CPA) has been used as a dysphoria-like behavior in animals. In mice β-arrestin2 deletion did not affect CPA induced by three KOR agonists [17]. In contrast, KOR-mediated CPA was reported to be mediated by GRK3-dependent p38 MAPK activation [18–21].

Recent studies revealed that GPCR signaling is cell-dependent; therefore, agonist in vitro functional selectivity from cell-based assays may not be extended to behavioral effects in animals and

Phosphoproteomic approach for agonist-specific signaling in mouse brains:…
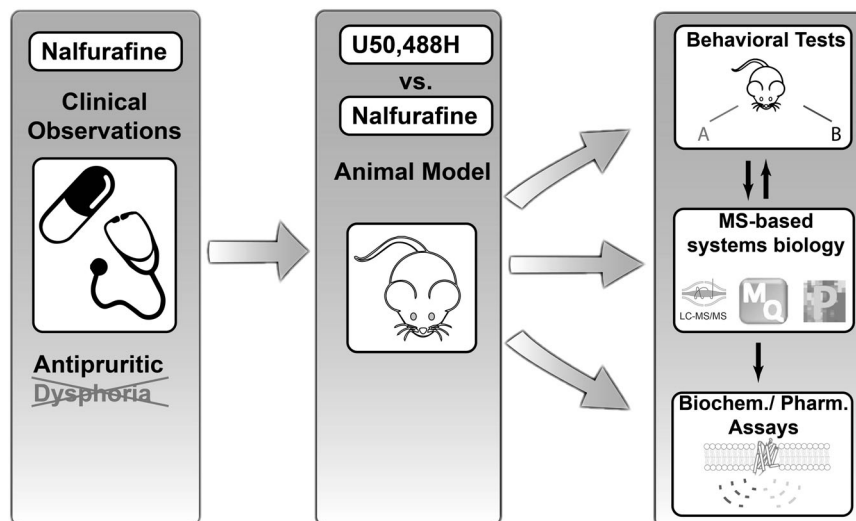JJ Liu et al.

940

Fig. 1 Overview of the "from Beside to Bench" strategy: Nalfurafine, the only KOR agonist in clinical use, has antipruritic effect without dysphoric effects and a very low rate of hallucinations, two side effects commonly associated with other KOR agonists. To investigate the biochemical mechanism, we established a mouse model to compare the effect of nalfurafine and U50,488H, a prototypic KOR agonist. This animal model enabled us to conduct mass spectrometry-based systems biology analysis. The insights obtained allowed us to generate and test hypothesis using behavioral tests, biochemical and pharmacological assays. This integrated strategy allowed us to bypass the in vitro model to generate insights that could impact on future drug discovery

in humans (reviewed in [15, 22]). As such, one of the immediate objectives in actualizing pathway-selective GPCR therapeutics is to develop approaches for evaluating ligand-specific signaling in vivo.

Herein we demonstrated that in mice nalfurafine did not cause CPA at doses effective for anti-scratch effects, mimicking clinical observations, whereas the opposite was observed for U50,488H and MOM-SalB. We thus formulated a "from-bedside-to-bench" approach to understand mechanisms underlying KOR-mediated aversion (Fig. 1). This approach bypasses the need of an in vitro cell-based system, by directly using mice as the platform for investigation. In particular, the recent break-throughs in MS-based phosphoproteomic [23–25] enabled us to obtain comprehensive phosphoproteomes of brain tissues, which allowed a detailed investigation of the molecular mechanisms of KOR actions. From such experiments, we obtained an unprecedented overview of KOR drug actions in various relevant brain regions. The combination of phospho-proteomics and pharmacologic approaches enabled us to predict and test signaling pathways involved in KOR-mediated aversion. This approach presents a novel path in discovery of GPCR-based therapeutics.

MATERIALS AND METHODS

Drugs
(±)U50,488H and nalfurafine were obtained from the National Institute on Drug Abuse (Bethesda, MD). MOM-SalB was provided by Dr. David Lee of McLean Hospital (Belmont, MA). Rapamycin was purchased from LC Laboratories (Woburn, MA). The vehicle for U50,488H and nalfurafine was saline, while that for MOM-Sal B and rapamycin was ethanol: Kolliphor EL:water (1:1:98) (veh-EK). Unless otherwise noted, KOR agonists, rapamycin and vehicles were injected subcutaneously (s.c.) in a volume of 0.1 ml/10 g body weight.

Materials
[^{35}S]GTPγS (1250 Ci/mmol) was purchased from PerkinElmer Life Sciences (Boston, MA). Mouse neuro2A neuroblastoma (N2A) cells were obtained from the ATCC (Manassas, VA). The following materials were purchase from Sigma-Aldrich (St. Louis, MO):

formalin, compound 48/80, Kolliphor EL, GDP and GTPγS. Phospho-p70 S6 Kinase (Thr389) (108D2) Rabbit mAb #9234, HRP-linked goat anti-rabbit IgG Antibody #7074, p70 S6 Kinase Antibody #9202 were from Cell Signaling Technology (Danvers, MA). Other commonly used chemicals were obtained from Sigma-Aldrich or ThermoFisher Scientific.

Animals and behavior tests
Adult male CD-1 mice (Charles River Laboratories, Wilmington, MA), 30–35 g, were used for most experiments. Adult male MOR knockout [26] and wildtype mice in C57BL/6 background (25–30 g) were used in some experiments. All procedures were approved by Temple University School of Medicine Institutional Animal Care and Use Committee.

Compound 48/80 scratching test was performed as we described [27]. Briefly, after acclimation to individual observation boxes for 1H, mice were injected with vehicle or a KOR agonist and 20 min later with 0.1 ml compound 48/80 (0.5 mg/ml, 50 µg, s.c) into the nape. Starting 1 min post-injection, the number of bouts of hind leg scratching the neck was counted for 30 min. The relative % reduction of scratching was calculated as follows:

$$\frac{\text{Mean number of scratches by control group} - \text{mean number of scratches by treatment group}}{\text{Mean number of scratches by control group}} \times 100\%$$

Formalin test was performed as described [28]. Briefly, after acclimation, mice were treated with vehicle or a KOR agonist and placed in glass jars (14 cm in diameter). Five minutes later, mice were mildly sedated with 3-5% isoflurane, injected s.c. with 5% formalin (20 µl) into the plantar region of the right hind paw, and returned to the jars. The time each animal licked/groomed the formalin-injected paw was recorded from 15 to 35 min post-injection (phase II reaction). The relative % antinociception was calculated as follows:

$$\frac{\text{Mean licking time of control group} - \text{Mean licking time of treatment group}}{\text{Mean licking time of control group}} \times 100\%$$

A_{50} values of KOR agonists in the anti-scratch and antinociception tests were determined by plotting dose against % anti-scratch or antinociception and using linear regression to obtain a best-fit line (Prism 6.0, GraphPad Software, La Jolla, CA).

Phosphoproteomic approach for agonist-specific signaling in mouse brains:…
JJ Liu et al.

941

Conditioned place aversion (CPA) is a rodent model of dysphoria. The procedure was adapted from our method of conditioned place preference (CPP) [29]. During the pre-test on Day 0, each animal roamed freely between the two chambers for 15 min and the time spent in each was recorded. An unbiased and counterbalanced design was used. In the conditioning phase (Days 1–6), two sessions/day were conducted, with ≥4H in between. Injections of vehicle and a KOR agonist were carried out in the morning and afternoon sessions, respectively. After each injection, the mouse was placed in the home cage for 15 min and then confined to one chamber for 30 min for conditioning. On the post-test day (Day 7), the animals again roamed freely between the two chambers for 15 min, and time spent on each side was recorded. The score was calculated by subtracting the pre-test time from the post-test time in the drug-paired chamber. A negative score indicates aversion, while a positive score indicates preference.

In the rapamycin experiments, from day 1 to 6, in the morning mice were injected with vehicle followed by 30 min later with saline before conditioning. In the afternoon, mice were pre-treated with rapamycin (5 mg/kg, on days 1, 3, 5) or vehicle for 30 min followed by U50,488H (5 mg/kg) or saline before conditioning.

Intracranial self-stimulation (ICSS) was performed on mice as described (Muschamp et al. 2011)[30]. Mice were stereotactically implanted with a monopolar stimulating electrode (PlasticsOne, Roanoke, VA) located in the medial forebrain bundle (from bregma: AP: -1.9, ML: $+0.8$, DV: -4.8 mm). After five days of recovery, mice were trained at the lowest current that would sustain responding at a rate of ~1 response/s (±10%; FR1 schedule of reinforcement). This preferred current was then maintained through testing in which mice were permitted 50 s to respond for one of fifteen stimulation frequencies (158–34 Hz). The minimum frequency at which stimulation supports operant responding was reward threshold or "θ_0". Drug testing began when reward thresholds reached a stable performance criteria (±10% for three consecutive days). For drug treatment sessions, U50,488H or nalfurafine were administered 45 min after beginning the task. Fifteen min later, thresholds were quantified from performance during 15-min test sessions. Percent baseline was computed as: (threshold after drug/threshold before drug) × 100.

Measurement of locomotor activities was performed according to our published procedures [29] using a Home Cage Locomotor Activity System (Omnitech Electronics Inc., Columbus, OH) and eight individual activity monitors. Mice were treated with saline, U50,488H (5 mg/kg) or nalfurafine (20 µg/kg) (2.5x A_{50} values in the anti-scratching test) and put into locomotor chambers right after injections. Activities were continuously monitored over a 60 min period.

Rotarod test was performed with procedures adapted from that of White et al. [17] using a mouse rotarod apparatus (Ugo-Basile, Stoelting Co., Wood Dale, IL). One day before the test, mice were trained to run on the rotarod for 5 min with the rotation revolution changing from 5 to 50 rpm. Each mouse was trained for 2–3 trials with a 1-min break between trials. Mice which could stay on the rotarod for >240 s (80% of the 5-min period) after training (~50% of mice) were used. One the test day, mice were tested on the rod first to measure baselines. The mice (>90%) having baseline >240 s were injected with a KOR agonist or saline. 10, 20, 30, and 40 min after injection, mice were repeatedly tested for the time staying on the rotarod for 5 min. Results are shown as % time staying on the rod following drug or vehicle administration compared with the baseline.

Phosphoproteomic analyses of the mouse brain regions following treatment with U50,488H and nalfurafine
CD-1 mice were injected with vehicle, U50,488H (10 µg/kg), or nalfurafine (30 µg/kg) ($n = 3$ each) and euthanized 30 min later.

Brain regions were dissected and solubilized in 4% SDS, 50mM Tris, pH 7.4 (40mg wet weight tissue /0.6ml) and stored at -20 °C until analysis. Phosphoproteomic sample preparation was described previously [24]. Samples were then measured using Thermo Scientific Qxactive HF orbitrap, and processed with Maxquant (version 1.5.5.2) [31]. The resulted data table was processed bioinformatically using R and Perseus (version 1.5.2.17) [32].

The annotation matrix algorithm was applied under the Perseus environment (version 1.5.0.1). Briefly, individual data set was normalized against the median of their respective control groups and was annotated with Gene ontology terms or KEGG pathways terms based on their protein identification. The annotation matrix is an expansion of 1D annotation enrichment described by Cox and Mann [33]. In brief, phosphosites of proteins in the one annotated category was tested against the remaining phosphosites through a Wilcoxon–Mann–Whitney U test. We then set p-value $= 0.001$ as the cutoff, and obtained the median differences between the significantly regulated category and the background. We then performed one sample t test on each experimental condition against 0.

The annotation matrix algorithm has been previously used in proteomic studies [33]. The rationale is that if a signaling pathway is activated by receptor-agonist interaction, phosphorylation changes in multiple members of this pathway will occur. Such perturbation will be statistically significant on the pathway as a whole, even if not at individual phosphorylation event. In addition, most phosphorylation events have not been characterized in the brain and this method brings the focus on the pathway level instead. For proteomics or phosphoproteomics studies that examine signaling pathways as a whole, it is a common practice to measure 3–4 biological replicates per condition [34–36].

Effects of U50,488H, rapamycin or both on p70S6K phosphorylation
Clonal N2A-FmK6H cells established previously [37] (see Supplementary Methods) were seeded in 24-well plates, grown to ~80% confluence and serum-starved overnight. Cells were washed with Minimum Essential Medium, incubated with rapamycin (40 nM) or vehicle for 30 min and U50,488H (10 µM), vehicle or fetal bovine serum (FBS) (10%) was added and incubated for another 10 min. P70S6K phosphorylation at T389 was detected by immunoblotting [37] with phospho-T389 p70S6K rabbit monoclonal antibodies followed by goat anti-rabbit IgG light chain conjugated with horseradish peroxidase and then reaction with Enhanced Chemiluminescence reagents. Images were captured and staining intensities of bands were quantitated using the ImageGauge software. The blots were stripped and re-blotted for total p70S6K. Images were captured and staining intensities of bands were quantitated. Intensity of p-T389 p70S6K was normalized against that of total p70S6K in the same lane and then the relative intensity was normalized against that of FBS.

RESULTS
While U50,488H, MOM-SalB and nalfurafine produced anti-scratch and analgesic effects, U50,488H, but not nalfurafine, promoted CPA, anhedonia, sedation and motor incoordination in mice
Each agonist dose-dependently inhibited compound 48/80-induced scratching behavior (Fig. 2a). U50,488H at 2.5 and 5 mg/kg, MOM-SalB at 0.05, 0.1, 0.2, and 0.3 mg/kg and nalfurafine at 5, 10, 20 and 30 µg/kg significantly reduced scratching behavior. The A_{50} values for nalfurafine, MOM-SalB and U50,488H were 8.0 µg/kg, 70.2 µg/kg, and 2.07 mg/kg, respectively, similar to those previously reported [27].

Each agonist also inhibited pain behaviors in the late phase of the formalin test (Fig. 2b) in a dose-dependent manner, with A_{50} values of 5.8 µg/kg, 17 µg/kg, and 0.58 mg/kg, respectively.

Phosphoproteomic approach for agonist-specific signaling in mouse brains:...
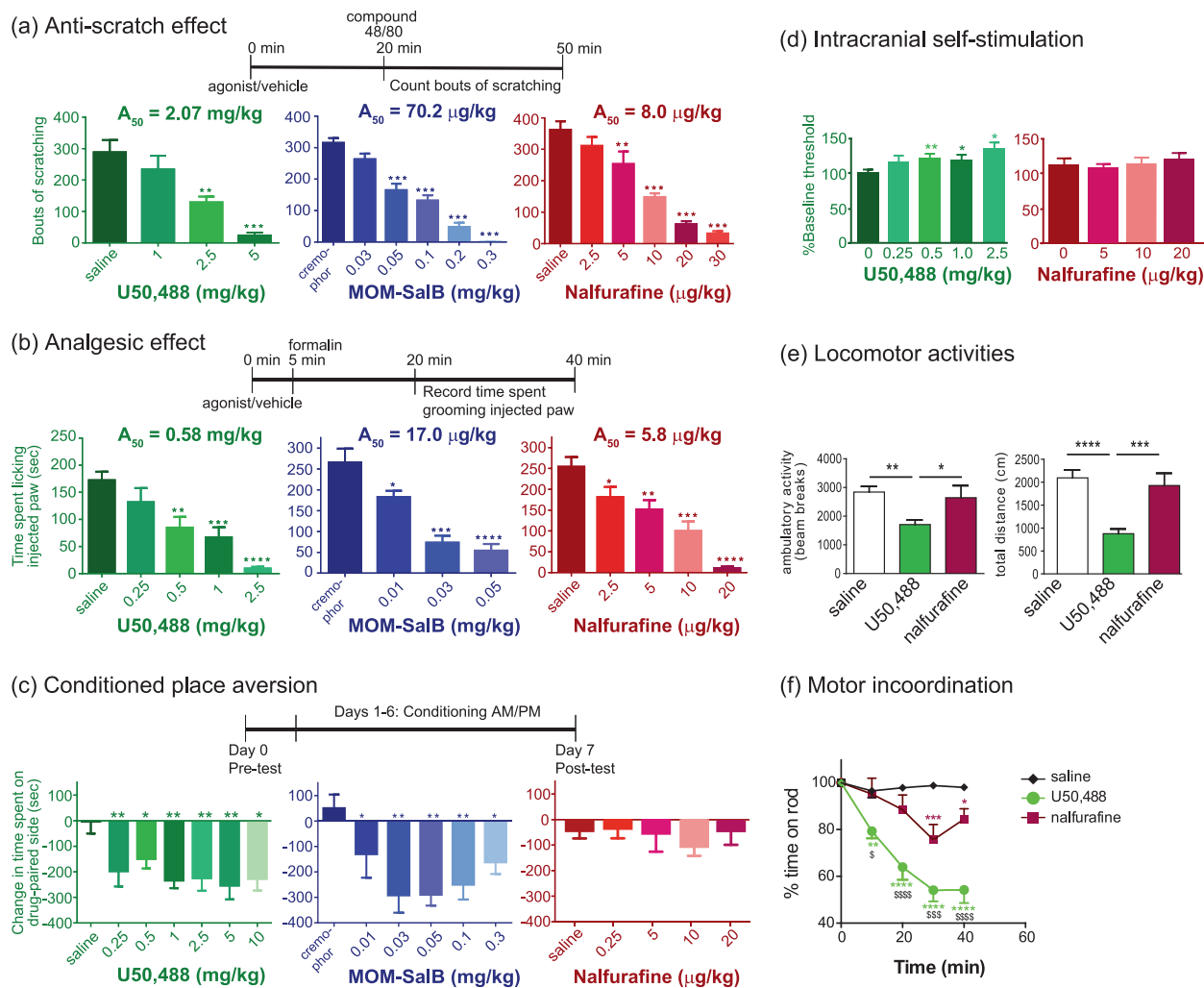JJ Liu et al.

942

Fig. 2 **a** KOR agonists inhibited scratching behavior induced by compound 48/80. Vehicle or one of the different doses of U50,488H, MOM-SalB or nalfurafine was injected (s.c.) 20 min before compound 48/80 and the bouts of scratching were counted for 30 min. A_{50} doses were determined as described in Methods. Data were analyzed using one-way ANOVA followed by Dunnett's post-hoc test. Results of one-way ANOVA were: U50,488H, $F(3,29) = 14.12$, $p < 0.0001$; MOM-SalB, $F(5,42) = 57.18$, $p < 0.0001$; nalfurafine, $F(5,44) = 31.04$, $p < 0.0001$. Significance levels are **$p < 0.01$, ***$p < 0.001$, compared to vehicle control by Dunnett's post-hoc test (mean ± SEM, $n = 8$–10 animals/group). **b** KOR agonists inhibited formalin-induced pain behaviors. Vehicle or one of several doses of U50,488H, MOM-SalB or nalfurafine was injected (s.c.) 5 min before formalin and the amount of time the animal spent licking the injected paw was counted for 20 min starting ~15 min after formalin injection. A_{50} doses were determined as described in Methods. Data were analyzed using one-way ANOVA followed by Dunnett's post-hoc test. Results of one-way ANOVA are: U50,488H, $F(4,41) = 11,43$, $p < 0.0001$; MOM-SalB, $F(3,32) = 21.13$, $p < 0.0001$; nalfurafine, $F(4, 41) = 18.65$, $p < 0.0001$. Significance levels are *$p < 0.05$, **$p < 0.01$, ***$p < 0.001$, and ****$p < 0.0001$, compared to vehicle control, from Dunnett's post-hoc test (mean ± SEM, $n = 8$–10 animals/group). **c** Conditioned place aversion (CPA) produced by U50,488H, MOM-SalB and nalfurafine. On Day 0, mice were subject to pre-test. On Days 1–6, KOR agonists were injected with vehicle or one of the various doses of U50,488H, MOM-SalB or nalfurafine 15 min before each 30-min conditioning session (2 sessions/day) for 6 days. On Day 7 (post-test), the length of time the animal spent on the drug-paired side was measured. The graph shows the time the animal spent during the post-test subtracting the amount of time spent during the pre-test. Results of one-way ANOVA are: U50,488H, $F(6,56) = 3.738$, $p = 0.0034$; MOM-SalB, $F(5,53) = 5.318$, $p = 0.0005$; nalfurafine, $F(4,47) = 0.3811$, $p = 0.8210$. Significance levels are *$p < 0.05$, **$p < 0.01$, compared to vehicle control (mean ± SEM, $n = 8$–10 animals/group) by Dunnett's post-hoc test. **d** Effects of U50,488 and nalfurafine on % change in baseline reward threshold in ICSS. Vehicle or one of the different doses of either drug was injected and 15 min later thresholds were measured. Data are mean ± S.E.M. ($n = 12$/group). Results of repeated measures one-way ANOVA revealed a significant main effect of U50,488H dose on baseline threshold [$F(4,30) = 5.029$, $p < 0.01$]. **$p < 0.01$ and *$p < 0.05$, compared to the control group by Dunnett's post-hoc multiple comparisons test. **e** Effects of U50,488 and nalfurafine on novelty-induced locomotor activity. Mice were treated s.c. with saline, U50,488H (5 mg/kg) or nalfurafine (20 µg/kg) (2.5x A_{50} values in the anti-scratching test) and total locomotor activities were monitored. Cumulative data between 0 and 30 min post-injection are shown here. Each value represents mean ± SEM ($n = 8$–12). Ambulatory activity: **$p < 0.01$, *$p < 0.05$, compared with the U50,488H group by one-way ANOVA [$F(2,27) = 6.254$, $p = 0.0059$] followed by Tukey post-hoc test. Total distance: ***$p < 0.001$, ****$p < 0.0001$, compared with the U50,488H group by one-way ANOVA [$F(2, 29) = 15.61$, $p < 0.0001$] followed by Tukey post-hoc test (**f**) Effects of U50,488H and nalfurafine on motor coordination on the rotarod test. After training the previous day, mice were injected s.c. with saline, U50,488H (5 mg/kg) or nalfurafine (20 µg/kg) and tested on the rotarods 10, 20, 30, and 40 min after injection. The time each stayed on the rods was recorded and normalized against the baseline. Data were analyzed with 2-way ANOVA followed by Tukey's multiple comparisons test (mean ± SEM, $n = 9$ or 10/group). Results of two-way ANOVA showed a significant main effect of treatment [$F(2,130) = 65.2$, $p < 0.0001$], a significant main effect of time [$F(4,130) = 17.32$, $p < 0.0001$] and a significant interaction [$F(8,130) = 6.343$, $p < 0.0001$]. *$p < 0.05$, **$p < 0.01$, ***$p < 0.001$, ****$p < 0.0001$, compared with saline group; $$p < 0.05$, $$$p < 0.001$, $$$$p < 0.0001$, compared with the nalfurafine group, by Tukey's post-hoc test

Phosphoproteomic approach for agonist-specific signaling in mouse brains:...
JJ Liu et al.

943

U50,488H at 0.5, 1.0, 2.5 mg/kg, MOM-SalB at 0.01, 0.03, 0.05 mg/kg and nalfurafine at 2.5, 5, 10, 20 µg/kg significantly reduced pain behavior.

In the CPA test, all the doses tested of U50,488H (0.25–10 mg/kg) or MOM-SalB (0.01–0.3 mg/kg) produced significant aversion, compared to vehicle (Fig. 2c). Curiously, the effect was not dose-dependent for either drug. In contrast, nalfurafine (Fig. 2c) did not produce significant aversion at 2.5, 5, 10, or 20 µg/kg. U50,488H at 0.25, 0.5, 1, 2.5, 5, 10 mg/kg and MOM-SalB at 0.01, 0.03, 0.05, 0.1, 0.2, and 0.3 mg/kg caused significant CPA.

Thus, MOM-SalB and U50,488H were aversive at doses that are much lower than the A_{50} values for anti-scratch and antinociception. However, nalfurafine did not produce significant aversion at a dose that is 2.5-fold of the A_{50} in the anti-scratch test (Table S1).

In vitro selectivity of nalfurafine for the KOR over MOR ranges from 15 to 69 and nalfurafine is a full agonist at the KOR and a partial agonist at the MOR [27, 38]. The inability of nalfurafine to induce CPA may be due to its action on the MOR that produces conditioned place preference, which counteracts KOR-induced CPA. To test this possibility, CPA was performed in MOR−/− mice. As shown in Fig. S2a, nalfurafine (10 µg/kg) did not cause CPA in either the wildtype or MOR−/− mice, whereas 10 µg/kg nalfurafine inhibited compound 48/80-induced scratch by ~50% in MOR−/− mice (Fig. S2b). These results indicate that nalfurafine at the dose we used does not act on the MOR.

In the ICSS test, compared with the control, U50,488H at 0.5, 1.0, and 2.5 mg/kg significantly increased baseline threshold, consistent with previous results [39], whereas nalfurafine up to 20 µg/kg did not (Fig. 2d). Neither drug altered the % maximum rate (not shown). Thus, U50,488H, but not nalfurafine, produced anhedonia without interfering with physical response capabilities. These results are consistent with the CPA results.

Inhibition of novelty-induced locomotion has been used as an indicator of sedation. U50,488H at 5 mg/kg showed significant inhibition, whereas nalfurafine at 20 µg/kg did not (Fig. 2e). The rotarod test was employed to measure motor incoordination. U50,488H at 5 mg/kg significantly reduced the time mice stayed on the rod at 10, 20, 30, and 40 min after drug administration, but nalfurafine at 20 µg/kg only had a small effect at 30 and 40 min following drug injection (Fig. 2f). The doses used are 2.5× A_{50} values in the anti-scratching test.

System view of phosphorylation events promoted by nalfurafine and U50,488H in mouse brains

A large-scale comparative high-throughput single-shot label-free MS-based phosphoproteomics study of KOR ligand in vivo effects was used for the survey of KOR signaling in different brain regions and the search of underlying mechanism of KOR-mediated aversion. Because MOM-SalB yielded similar CPA results as U50,488H, we compared only U50,488H and nalfurafine.

Mice were treated with U50,488H or nalfurafine at doses that reflect the behavioral differences shown above. Phosphoproteomics was performed on the cortex, hippocampus, striatum, spinal cord, and cerebellum. The mouse cerebellum has little or no detectable KOR expression [40], and is therefore used as a
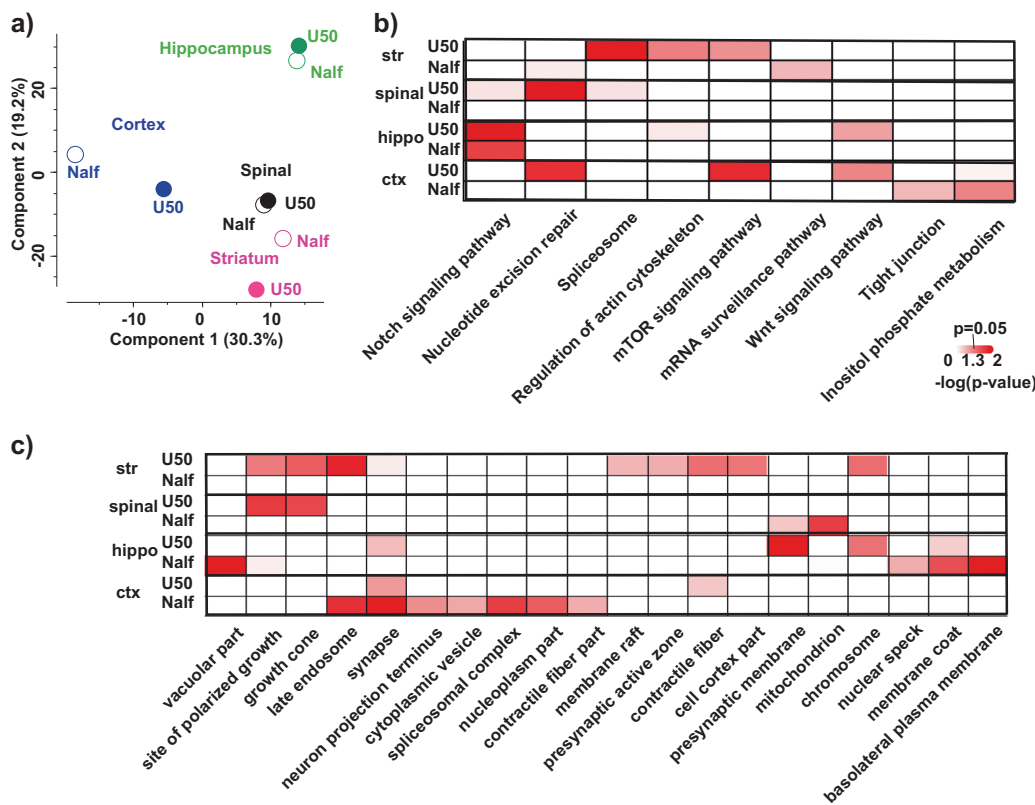
Fig. 3 Comparison of nalfurafine and U50,488-induced phosphoproteomic changes in brain regions: Mice were injected (s.c.) with vehicle, U50,488H (10 mg/kg), or nalfurafine (30 µg/kg) (*n* = 3 each) and euthanized 30 min later. Brain regions were dissected for analysis as described in Methods. **a** Principal component analysis (PCA) of phosphoproteomic changes induced by U50,488 or nalfurafine. Each drug treatment experiment was measured in triplicates and normalized against respective saline control. The median value for each condition was used as inputs for PCA; **b** Heatmap of annotation matrix analysis. Normalized drug treatment as described in **a** was used as inputs for annotation matrix analysis. Details are described in Methods. Kyoto Encyclopedia of Genes and Genomes (KEGG) pathway databased was used for the analysis. **c** Same as in **b** but gene ontology cellular component was used for the analysis

Phosphoproteomic approach for agonist-specific signaling in mouse brains:...
JJ Liu et al.

944

Fig. 4 KOR-mediated mTOR signaling in the brain: **a** a schematic drawing of mTOR signaling based on the KEGG pathway. U50,488-, but not nalfurafine-, regulated phosphoproteins in the cortex have been circled in red (also marked with *). "+p" indicates a kinase-substrate relationship. The dotted lines indicate indirect relationship, while the solid lines indicate direct interaction, with the arrow end indicating activation and blunt end indicating inactivation. It should be noted that activation of the mTOR pathway may occur in neurons expressing the KOR, those that do not express the KOR, but are downstream of KOR-containing neurons or both. **b** A heatmap of phosphoproteins and their sites that are annotated with "mTOR signaling pahtway" using KEGG. The p-value obtained from one-way ANOVA followed by Dunnett's post-hoc test with respective saline as controls was used to construct the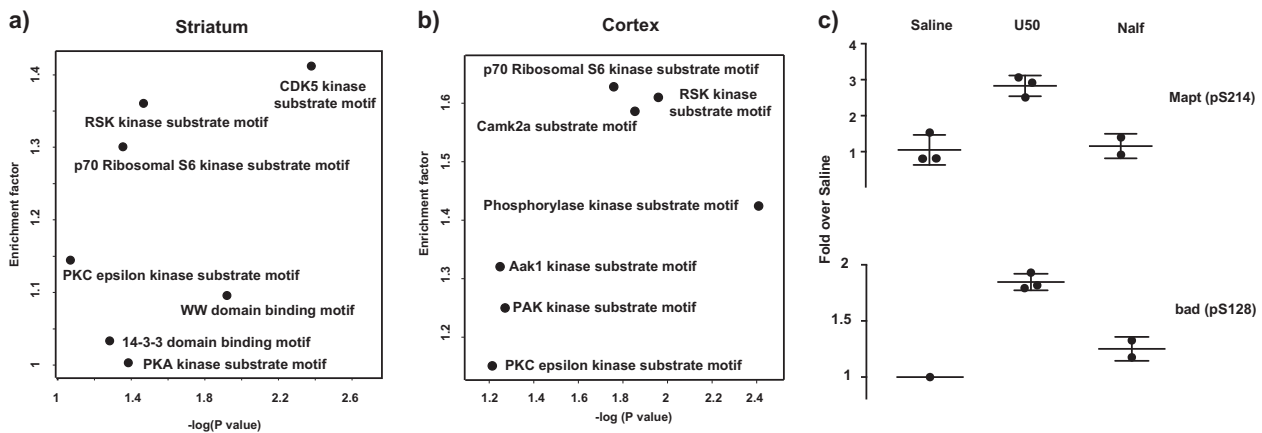 heatmap. The color code is shown top left, with a dotted line indicating the conventional 0.05 cutoff. An unsupervised hierarchical clustering was performed on phosphosites, indicated by the dendrogram on the left. The position of phosphosites on each protein are shown inside the parenthesis next to the gene name. "Nalf" indicates nalfurafine

negative internal control. As expected, fewer regulated sites were observed in the cerebellum than other brain regions (Fig. S3).

Over 50,000 phosphosites were quantified with average Pearson correlation ($r = 0.87$) among replicates within each experimental condition. We chose three biological replicates per experimental condition following the examples of phosphoproteomic studies of other systems [34, 35] and proteomic studies of the brain [36]. To understand the robustness of the present study, we performed Pearson correlation analysis of samples within each experimental condition and across different experimental conditions. We discovered that the Pearson correlation of samples within each condition is larger than those across different conditions ($p = 0.024$, unpaired, two-tailed Welch's t-test $t = 2.573$, df = 11.42) (Fig. S4). Furthermore, in each region, only about 5% phosphorylation events were perturbed by ligand stimulation, with U50,488H somewhat higher than nalfurafine (Fig. S5). Additionally, nalfurafine-induced phosphoproteome perturbation differed from U50,488H perturbation in a region-dependent manner. Using principal component analysis (PCA) to visualize the difference of drug actions in each brain region, the main discrepancy of nalfurafine-mediated and U50,488H-mediated effects resided in cortex and striatum (Fig. 3a), indicating that drug action is highly dependent on the brain region.

To further analyze the cellular locations and signaling pathways differentially impacted by U50,488H and nalfurafine in each brain region, we used the previously described annotation matrix algorithm [41]. The underlying principle of the annotation matrix algorithm is that phosphorylation changes disproportionally occur

in proteins annotated to the same cellular components or signaling pathways (Fig. S6). This approach circumvents the challenges that heterogeneous neuronal populations in brain yield changes of small magnitudes in comparison to cultured cell lines. We then applied hierarchical clustering, from which cellular components or signaling pathways preferentially activated by one drug (i.e., low p-value) group together. In accordance with the PCA analysis, the primary differences between nalfurafine and U50,488H were observed in the striatum and cortex (Fig. 3a). Particularly, in the striatum, cellular components such as "late endosome", "pre-synaptic active zone", and "chromosome" was preferentially impacted by U50,488H (Fig. 3c). On the pathway level, U50,488H also imposed different regulation from nalfurafine (Figs. 3b, S5). Two pathways may be particularly interesting: "mTOR signaling pathway" and "Wnt signaling pathway". mTOR signaling pathway was selectively affected by U50,488H in striatum and cortex, whereas the Wnt signaling pathway was selectively affected by U50,488H in hippocampus and cortex (Fig. 3b). We examined specifically the difference in drug actions in striatum and cortex. Close to 1000 and 480 phosphosites were found to be significantly regulated by at least one ligand treatment in cortex and striatum, respectively (one-way ANOVA with post-hoc Dunnett's test $p < 0.05$, a cutoff of 2×0.7 and 2×-0.7, equivalents of a minimal 60% increase and 40% decrease, respectively) (Supplementary Excel file). Within these phosphosites, we discovered a group of sites belonging to the mTOR pathway, which were significantly regulated by U50,488H, but not nalfurafine (Fig. 4b) in the striatum and cortex. U50,488H-promoted activation of the mTOR pathway may occur in KOR-

Phosphoproteomic approach for agonist-specific signaling in mouse brains:...
JJ Liu et al.

945

Fig. 5 Motif analysis results using the Fischer's exact test in **a** the mouse striatum and **b** the mouse cortex: The x-axis indicates the p-value of the motif enrichment, whereas the y-axis indicates the degree of the enrichment (1 = not enriched) (U50 vs. Nalf). In the Fischer's exact test, the background contains 12,172 phosphosites, in which 393 phosphosites denotes the difference between U50,488H and nalfurafine treatment as indicated in the text. The motif annotation was based on the consensus kinase substrate motif as indicated in the text. **c** U50,488H, but not nalfurafine, promoted phosphorylation of p70S6 kinase substrates Mapt and Bad in the striatum. The intensity of MS experiments was used in this analysis. Each data point was normalized against the average of saline samples. Each value is mean ± SD ($n = 3$, unless there was missing value in MS measurements) These phosphosites were indicated as p70S6 kinase substrates from the online database PhosphoSitePlus

expressing neurons, their downstream neurons through neuronal circuitry or both (Fig. 4a).

U50,488H and nalfurafine differentially regulate many phosphosites
A motif analysis, using the consensus kinase substrate motif [42, 43], was performed on ligand-dependent perturbation of phosphosites in the striatum and cortex. A Fischer's exact test was conducted on these phosphosites to examine the statistically significant over-representation of substrate motif in these phosphosites (Fig. 5a, b). The motif analysis of the phosphosites differentially regulated by the two agonists was further supported by different levels of phosphorylation of many proteins in the mTOR pathway in the striatum and cortex, but not much in the hippocampus and spinal cord. p70S6 kinase is downstream of mTOR and RSK impacts on the mTOR pathway. Phosphorylation of two of p70S6 kinase substrates, BAD (Bcl-2-associated death promoter protein) at S128 [44] and Mapt (Tau) at S214 [45] was increased by U50,488H, but not nalfurafine (Fig. 5c). The S6 ribosomal protein was not detected as being differentially regulated because of technical issues. As trypsin was used for digestion, the fragments generated from phosphorylated S6 will require multiple miscleavage events, which compromise the quantitation accuracy (R^{231}RR LpSpSLR ApSTSK pSESpSQR^{249}) [46]. These data indicate that the mTOR pathway may play an important role in the different signaling of nalfurafine and U50,488H. The mTOR signaling pathway has been implicated in depression both through direct drug actions and patients with severely depressive disorders [47, 48]. In addition, the mTOR pathway is the only one differentially regulated in both striatum (nucleus accumbens) and cortex (pre-frontal cortex), which constitute two of the most important brain regions in mood regulation through the mesolimbic and mesocortical pathways.

The mTOR inhibitor rapamycin abolished U50,488H-induced CPA, without affecting sedative, analgesic, and anti-scratch effects and motor incoordination
We next examined if the mTOR inhibitor rapamycin affected U50,488H-induced behaviors. Rapamycin can get into the brain with a half-life of ~48H [49, 50], so it was injected every other day (5 mg/kg, on days 1, 3, and 5) during 6-day conditioning. Treatment with rapamycin abolished U50,488H-induced CPA,

whereas rapamycin alone did not cause CPA or CPP (Fig. 6a). In contrast, rapamycin (30 min) did not affect U50,488H-induced sedative, anti-scratch, and analgesic effects and motor incoordination (Fig. 6b–e). Neither did pretreatment of rapamycin for 3H (not shown). Rapamycin alone had no effect in these tests. These results indicate that the mTOR pathway is involved in U50,488H-induced CPA, but not sedative, analgesic or anti-scratch effect or motor incoordination.

We then examined if the mTOR pathway was involved in MOM-SalB-induced CPA. Pretreatment with rapamycin (5 mg/kg) significantly reduced CPA promoted by MOM-SalB (0.05 mg/kg) (Fig. 6a), suggesting that the mTOR pathway may have a general role in KOR-mediated CPA.

U50,488H-promoted activation of the mTOR pathway in the brain may occur in KOR-expressing neurons, their downstream neurons through neuronal circuitry or both. We examined if U50,488H promoted p70S6K phosphorylation in the striatum by immunoblotting with antibodies against phospho-T389 p70S6K and total p70S6K. We found that the Mr of phospho-T389 p70S6K was ~85 kDa, presumably p85S6K, whereas that of total p70S6K was ~70 kDa (Fig. S7), making it difficult to interpret the data. We thus used N2A-FmK6H cells as a model of KOR-expressing neurons. U50,488H enhanced phosphorylation of p70S6K at T389 with an Mr of ~70 kDa, which was abolished by pretreatment with rapamycin, and the total p70S6K also had an Mr of ~70 kDa (Fig. 6f). As a positive control, 10% fetal bovine serum (FBS) greatly increased phosphorylation of p70S6K at T389, which was blocked by rapamycin. These results indicate that KOR activation can directly activate the mTOR pathway. However, mTOR activation may also happen in neurons downstream of KOR-containing neurons.

DISCUSSION
This study showcased the "from-bedside-to-bench" approach to discern the biochemical mechanisms underlying dysphoria/aversion caused by KOR agonists. The synergy between the mouse model, which captures important aspects of the clinical observations, and the large-scale MS-based phosphoproteomics is powerful in generating hypothesis for testing that can either point to new drug target or establish a platform for drug screen. The current study is also among the first to provide
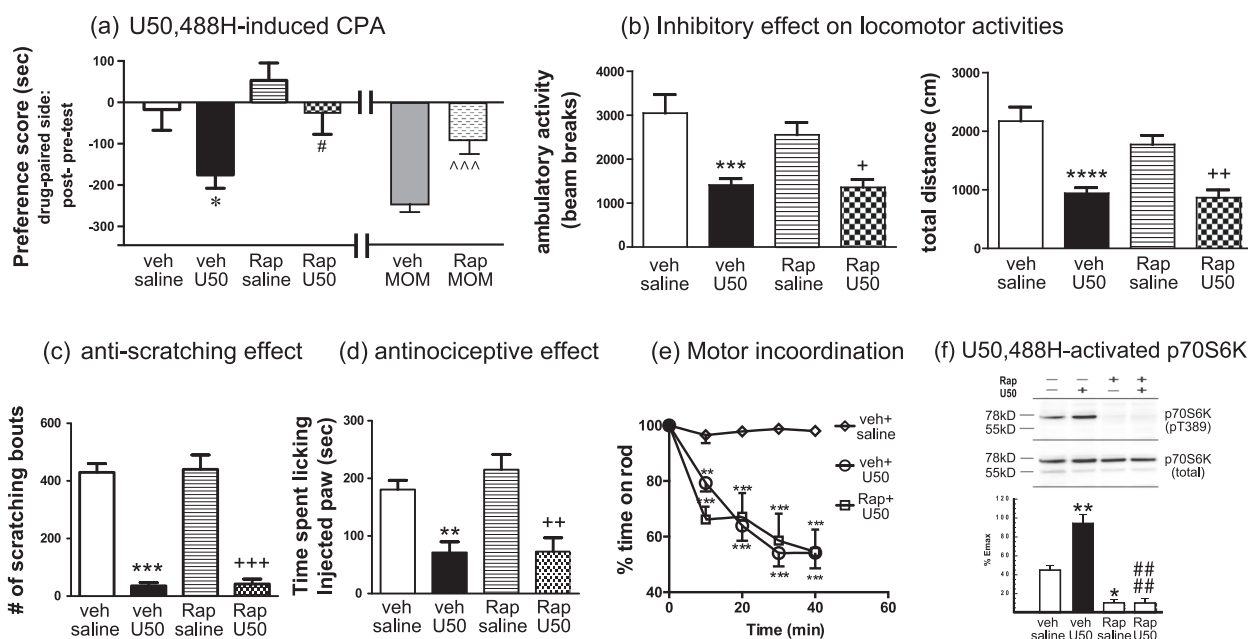
Phosphoproteomic approach for agonist-specific signaling in mouse brains:...
JJ Liu et al.

946

Fig. 6 Treatment with the mTOR inhibitor rapamycin blocked U50,488H-induced CPA without affecting its sedative, analgesic and anti-scratch effects. **a** For CPA, male adult CD-1mice were injected with vehicle or rapamycin (5 mg/kg, s.c.) 30 min before administration of saline, U50,488H (5 mg/kg) or MOM-SalB (50 μg/kg) on days 1, 3, and 5 during conditioning. For U50,488H-induced CPA, data were analyzed with two-way ANOVA followed by Sidak's multiple comparisons post-hoc test (mean ± SEM, $n = 10$/group). Results of two-way ANOVA showed a significant main effect of U50,488H treatment [F (1,36) = 6.917, $p = 0.0125$] and a significant main effect of rapamycin pretreatment [F (1,36) = 6.022, $p = 0.0191$], but no interaction [F (1,36) = 0.7855, $p = 0.3813$]. *$p < 0.05$, compared with vehicle/saline group; #$p < 0.05$, compared to vehicle/U50,488H group by Sidak's post-hoc test. For MOM-SalB-induced CPA, data were analyzed with unpaired t test ($t = 4.36$, df = 15). Each value is mean ± S.E.M ($n = 8$ or 9).^^^$p < 0.001$, compared with vehicle/MOM-SalB. For **b–e**, mice were injected with rapamycin (5 mg/kg, s.c.) or vehicle and kept in home cages and 30 min later injected with the vehicle or U50,488H (1 mg/kg, s.c. in the formalin test; 5 mg/kg, s.c. in the other tests). Experiments were then conducted as described in Fig. 2. **b** For inhibition of novelty-induced locomotor activity, data were analyzed with two-way ANOVA followed by Tukey's multiple comparisons post-hoc test (mean ± SEM, $n = 9$ or 10/group). Ambulatory activity: Results of two-way ANOVA showed a main effect of U50,488H treatment [F(1.34) = 27.48, $p < 0.0001$], but no main effect of rapamycin treatment [F(1,34) = 1.038, $p = 0.3155$] and no interaction [F(1,34) = 0.647, $p = 0.4268$]. *** $p < 0.001$ compared with vehicle/saline group; +$p < 0.05$ compared to Rap/saline group. Total distance: Results of two-way ANOVA showed a main effect of U50,488H treatment [F (1, 34) = 39.9, $p < 0.0001$], but no main effect of rapamycin treatment [F (1,34) = 1.216, $p = 0.2778$] and no interaction [F (1,34) = 0.9176, $p = 0.3449$]. ****$p < 0.0001$ compared with vehicle/saline group; ++$p < 0.01$ compared to Rap/saline group. **c** For inhibition of compound 48/80-induced scratching, data were analyzed with two-way ANOVA followed by Tukey's multiple comparisons *post-hoc* test (mean ± SEM, $n = 9$ or 10/group). Results of two-way ANOVA showed a main effect of U50,488H treatment [F(1, 34) = 176, $p < 0.0001$], but no main effect of rapamycin treatment [F(1,34) = 0.08024, $p = 0.7787$] and no interaction [F(1,34) = 0.003076, $p = 0.9561$]. ***$p < 0.001$, compared with vehicle/saline group; ###$p < 0.001$, compared to Rap/saline group. **d** for analgesic effect in the formalin test, data were analyzed with two-way ANOVA followed by Tukey's multiple comparisons post-hoc test (mean ± SEM, $n = 8$–10/group). Results of two-way ANOVA showed a main effect of U50,488H treatment [F(1,32) = 32.88, $p < 0.0001$], but no main effect of rapamycin treatment [F(1,32) = 0.6782, $p = 0.4170$] and no interaction [F(1,32) = 0.5623, $p = 0.4588$]. **$p < 0.01$, compared with vehicle/saline group; ###$p < 0.001$ compared to Rap/saline group. **e** for motor incoordination in the rotarod test, data were analyzed with 2-way ANOVA followed by Tukey's multiple comparisons test (mean ± SEM, $n = 9$ or 10/group). Results of two-way ANOVA showed a main effect of treatment [F (2,130) = 62.22, $p < 0.0001$], a main effect of time [F (4,130) = 21.29, $p < 0.0001$] and a significant interaction [F (8,130) = 5.489, $p < 0.0001$]. **$p < 0.01$, ***$p < 0.001$, compared with vehicle + saline group Tukey's post-hoc test. **f** Rapamycin inhibited U50,488H-promoted phosphorylation of p70S6K at T389 in N2A-FmK6H cells. Cells were grown in 24-well plates, serum-starved overnight, incubated with rapamycin (40 nM) or vehicle for 30 min and U50,488H (10 μM), vehicle or 10% fetal bovine serum (FBS) was added for another 10 min. P70S6K phosphorylation at T389 was detected with immunoblotting. The blots were stripped and re-blotted for total p70S6K. Intensity of p-T389 p70S6K was normalized against that of p70S6K and then the relative intensity was normalized against that of FBS. Data were analyzed by two-way ANOVA followed by Tukey's post-hoc test (mean ± SEM, $n = 3$ each). Results of two-way ANOVA showed a main effect of U50,488H treatment [F(1,8) = 17.09, $p = 0.0033$], a main effect of rapamycin treatment [F(1,8) = 99.05, $p < 0.0001$], and a significant interaction [F(1,8) = 17.09, $p = 0.0031$]. *$p < 0.05$, **$p < 0.01$compared with VehSal, ####$p < 0.0001$, compared with VehU50, by Tukey's post-hoc test

comprehensive phosphoproteomic analysis in brains following GPCR activation with unprecedented coverage and quantitation, which opens avenues for analysis of signaling of GPCRs and pathways involved in behaviors. This strategy, with no *a priori* assumptions, can circumvents the challenges of translating in vitro results on biased agonists into in vivo effects [15, 22] and opens the door for understanding in vivo GPCR pharmacology at a systems biology level. Notably, the mTOR pathway was found to be involved in KOR-induced CPA for the first time. Our results suggest that the ability of KOR agonists to activate mTOR pathway

in the striatum or cortex may provide a method to screen for KOR agonists devoid of aversive effects. This approach can be generally used for studying GPCR ligand-specific signaling.

Dose separation for nalfurafine between antinociception and CPA
Our results that nalfurafine at ≤20 μg/kg did not cause CPA and that there is dose separation between antinociception/anti-scratch and CPA for nalfurafine are consistent with published reports in ddY mice and in rats [51, 52]. Nalfurafine at 20 μg/kg caused lower motor incoordination in the rotarod test, in accord with the

Phosphoproteomic approach for agonist-specific signaling in mouse brains:…
JJ Liu et al.

947

finding of Endoh et al. [51]. In ICSS, we found that nalfurafine at 5, 10, or 20 μg/kg did not affect baseline threshold; however, Lazenka et al. [53], reported that nalfurafine at ≥10 μg/kg decreased rates of responding in Sprague–Dawley rats. The difference may be due to different species used. Since nalfurafine at 20 μg/kg did not affect motor activity, its antinociceptive and anti-scratch effects are not due to reduced motor activity. Our observations in CD-1 mice are different from those of Lazenka et al. [53] in rats.

One possibility why nalfurafine did not elicit CPA, sedation and motor incoordination may be due to its inability to get into the brain. However, previous studies have demonstrated that this is not the case. Systemic nalfurafine inhibits intrathecal or intracisternal morphine-induced scratching [54, 55]. The anti-scratch activity of s.c. nalfurafine was antagonized by i.c.v. norBNI [55]. The results shown in Fig. 3 demonstrated that in brain regions some pathways and subcellular organelle molecules were activated by nalfurafine, but not U50,488H, indicating its ability to get into the brain.

Another possibility is that nalfurafine may act on targets besides the KOR. Here we showed that lack of CPA by nalfurafine was not due to its action on the MOR (Fig. S2). Analgesic and anti-scratch effects of nalfurafine (20–200 μg/kg, s.c.) were inhibited by norBNI, but not by a MOR or DOR antagonist, indicating its effects are KOR-mediated [51, 56, 57]. Thus, at the doses we used (2.5–20 μg/kg, s.c.), nalfurafine is selective for the KOR. In vitro screening revealed that nalfurafine at 10 μM did not bind significantly to 45 pharmacological targets, nor did it affect release of several inflammatory mediators (Supplementary note) [12].

Since both U50,488H and MOM-SalB caused CPA at doses lower than those effective in the antinociception and anti-scratch tests, we reasoned that if the lack of CPA by nalfurafine was due to actions on the MOR, it would have caused CPA at a relatively low dose in MOR−/− mice, which was why we used 10 μg/kg nalfurafine in the CPA test. For the rotarod and locomotor activity experiments, we used a dose (20 μg/kg) higher than the A_{50} values of nalfurafine in the anti-scratch (8.0 μg/kg) and antinociception (5.8 μg/kg) tests, to ascertain that there was dose separation between antinociception and anti-scratch effect vs. motor incoordination and hypolocomotion. Our behavior results indicate that nalfurafine is fundamentally different from U50,488H; therefore, we used a higher dose (30 μg/kg) in the phosphoproteomics study.

Phosphoproteomic analysis
Shotgun phosphoproteomic experiments provided a system-wide view of changes in downstream phosphorylation events upon KOR activation at the early time points (up to 30 min). The changes in phosphoproteome provide a tool to generate hypothesis for the signaling pathways that lead to the eventual behavioral response. The recent advances in MS-based proteomics [23] enabled comprehensive coverage and accurate quantification of tens of thousands phosphosites simultaneously. In particular, the EasyPhos technology [24] permitted parallelization of sample preparation, such that hundreds of phosphoproteomic experiments were measured without sacrificing the depth of coverage or quantification accuracy.

The number of biological replicates in the phosphoproteomic experiments differs from behavioral experiments due to the nature of bioinformatic analysis. The advancement in the quantitative power of mass spectrometry and bioinformatics analysis have enabled comparative studies of drug actions in the brain. This is evident in the robust quantification within experimental conditions (higher Pearson correlation within experimental condition than between). Furthermore, the annotation matrix approach allows for comparison at the pathway level. Each signaling pathway contains more than twenty independent phosphorylation events, boosting the statistical power of comparison. We found that six component proteins of the mTOR pathway were differentially phosphorylated by the two agonists (Fig. 4a),

indicating that this pathway is differentially regulate. Since these changes in phosphoproteins were independently measured, the statistic power is greater than that from a single observation, such as a particular behavioral response. Lastly, the hypotheses generated based on phosphoproteomic observations were validated at biochemical and behavioral levels.

The differences in activation between high CPA-producing U50,488H and no CPA-producing nalfurafine should be reflected in the perturbation of downstream phosphoproteome. Phosphoproteomics studies on GPCR signaling have been performed on cultured cells [for example [58, 59]]. To the best of our knowledge, this study and that of Liu et al. [60] are the first two performed on brains. One of the most prominent discoveries is that nalfurafine and U50,488 induces different perturbation in different brain regions (Fig. 3), demonstrating that a complex environment of in vivo pharmacology.

Involvement of the mTOR pathway in KOR-mediated CPA
mTOR complex 1 activates p70S6 kinase, which in turn increases phosphorylation of the ribosomal protein S6, leading to increased protein synthesis. We showed that the mTOR pathway was activated to higher degrees by U50,488H than by nalfurafine in the striatum and cortex. The mTOR inhibitor rapamycin blocked U50,488H-induced and MOM-SalB-induced CPA, demonstrating for the first time that the mTOR pathway is involved in KOR-mediated CPA. Consistent with our finding is a recent study that the mTOR pathway in the striatum and cortex of C57BL/6 mice was differentially regulated by intracerebroventicular administration of U50,488H, which caused CPA, and 6′-GNTI, which did not cause CPA [60]. Thus, the ability of KOR agonists to activate the mTOR pathway may be used as a method to distinguish high and low CPA-producing KOR agonists. Although mTOR inhibition abolished KOR-mediated aversion, addition of rapamycin or any other mTOR inhibitor to a KOR agonist for therapeutic use is not advised since mTOR inhibitors have anticancer and immunosuppressant effects (https://www.accessdata.fda.gov/drugsatfda_docs/label/2015/021083s058,021110s075lbl.pdf).

The mTOR pathway has been implicated in learning and memory. However, rapamycin had no effect on cocaine CPP when given prior to each conditioning session [61], excluding the possiblility that abrogation of U50,488-induced CPA by rapamycin is due to its inhibition on learning and memory during conditioning.

Activation of the mTOR pathway and the subsequent increases in synaptic protein synthesis and synapse formatin in the rat prefrontal cortex have been implicated in rapid-acting antidepressant effects of ketamine [48, 62]. Our findings raise many questions about the mTOR pathway and KOR-mediated CPA: are mTOR-mediated increased synaptic protein synthesis and synaptic formation are involved in CPA? Are the two p70S6 kinase substrates Mapt and BAD, which were differentially phosphorylated by U50,488H and nalfurafine, participate in CPA induced by U50,488H? In what brain nuclei and specific neurons does mTOR activation occur following KOR activation? Does mTOR activation happen in KOR-containing neurons. These questions remain to be investigated.

p38 MAPK activation in the VTA and raphe nucleus have been implicated in CPA induced by KOR agonists [18, 19, 21]. KOR activation enhanced p38 MAPK phosphorylation in primary mouse striatal neurons and astrocytes [20] and in mouse striatum [19]. However, in our phosphoproteomics measurements, we did not consistently observe phosphorylation of the p38 MAPK signaling pathway following U50,488H. Changes of phosphorylation levels are dynamic and transient. Therefore, it is possible that p38 phosphorylation may occur at a time point not captured in the current study.

It is likely that multiple signaling pathways in different brain regions are involved in KOR-mediated CPA. This notion is supported by the observation that several other pathways were

Phosphoproteomic approach for agonist-specific signaling in mouse brains:...
JJ Liu et al.

948

differentially regulated by U50,488H and nalfurafine (Fig. 3). Some of these pathways, including the Wnt pathway, may be involved in CPA. Here we chose to study the mTOR pathway for three reasons. It is the only pathway differentially regulated in the cortex and striatum, two regions important in mood regulation. In addition, it is involved in emotional response and synaptic protein regulation. Furthermore, there are readily available inhibitors of this pathway. The other differentially regulated signaling pathways will be investigated in future studies.

Interestingly, even though U50,488H, but not nalfurafine, caused significant sedation and motor incoordination, inhibition of the mTOR pathway did not affect these behaviors, indicating that other signaling pathway(s) is(are) involved in these effects. Prototypic KOR agonists cause hallucinations. It should be noted that none of the behaviors examined here is a model or test for hallucinations. Mechanisms underlying this behavior remain to be investigated.

In vivo and in vitro differences
Nalfurafine clearly produced different behavioral effects in vivo from U50,488H and MOM-SalB. In contrast, we did not observe G protein-dependent or arrestin-dependent functional selectivity in vitro. We found that U50,488H, nalfurafine and MOM-SalB were full agonists in promoting KOR-mediated [^{35}S]GTPγS binding to membranes of N2A-FmK6H cells with EC_{50} and E_{max} values shown in Table S2. In addition, nalfurafine induced recruitment of β-arrestin1 or 2 dose-dependently with high potency and to levels comparable to U50,488H and/or MOM-SalB in HEK293 cells expressing mKOR-donor and β-arrestin1- or 2-acceptor using β-galactosidase complement assay (Table S3). When the bias factor of U50,488H was set at 1, nalfurafine did not show a bias factor different from U50,488H (Table S4). Schattauer et al. [63] recently reported that nalfurafine was a G protein-biased KOR agonist in HEK293 cells using ERK1/2 and p38 MAP kinase phosphorylation as functional end points of G protein-dependent and β-arrestin-dependent pathways, respectively. Thus, there are system and end-point-dependent results in vitro. This, therefore, highlights the importance of studying brains directly. As reviewed previously [15, 22], many factors may contribute to the disconnect between in vitro and in vivo results, including heterogeneity of neurons and glias in the brain, complex involvement of neuronal circuitry, receptor expression levels, cellular components involved in receptor phosphorylation and signaling (GRKs, β-arrestins, and downstream effectors).

Biased KOR signaling in behaviors
G protein and β-arrestin2-biased signaling was linked to KOR-mediated behaviors. β-arrestin2 deletion impaired KOR-mediated motor incoordination [17], demonstrated involvement of β-arrestin2 in this behavior, but did not affect antinociception, hypolocomotion, CPA, or anti-scratch effect [17, 64]. Studies have also been done on KOR agonists shown to be G protein-biased in cultured cells, including RB-64 [17] and triazole 1.1 [65]. RB-64 produced antinociception and CPA without causing motor incoordination, sedation and anhedonia in the ICSS test. Triazole 1.1 produced analgesic and anti-pruritic effects without causing sedation, reduction in dopamine release or anhedonia. Nalfurafine exhibits analgesic and anti-scratch effects, but causes no CPA, anhedonia, motor incoordination or sedation. Thus, KOR agonists may share some pharmacological effects, but also show individual differences.

AUTHOR CONTRIBUTIONS
Perform phosphoproteomics experiments and analyze data: J.J.L., M.M. design and perform animal treatment, behavioral experiments and analyze data: Y.T.C., K.M.D., C.C., P.H., T.A.G., J.W.M., A.C. and L.-Y.L.-C. Write manuscript: J.J.L., L.-Y.L.-C., Y.-T.C., P.H. provide inputs to manuscript: M.M., C.C., K.M.D.

ADDITIONAL INFORMATION

REFERENCES
1. Cowan A, Kehner GB, Inan S. Targeting Itch with ligands selective for kappa opioid receptors. Handb Exp Pharmacol. 2015;226:291–314.
2. Ansonoff MA, Zhang J, Czyzyk T, Rothman RB, Stewart J, Xu H, et al. Antinociceptive and hypothermic effects of Salvinorin A are abolished in a novel strain of kappa-opioid receptor-1 knockout mice. J Pharmacol Exp Ther. 2006;318:641–8.
3. Lemos JC, Chavkin C. Kappa opioid receptor function. In: Pasternak GW editors. The opiate receptors, 2nd ed. Humana Press; 2011. p. 265–306.
4. Pfeiffer A, Brantl V, Herz A, Emrich HM. Psychotomimesis mediated by kappa opiate receptors. Science. 1986;233:774–6.
5. Roth BL, Baner K, Westkaemper R, Siebert D, Rice KC, Steinberg S, et al. Salvinorin A: a potent naturally occurring nonnitrogenous kappa opioid selective agonist. Proc Natl Acad Sci USA. 2002;99:11934–9.
6. Simonin F, Valverde O, Smadja C, Slowe S, Kitchen I, Dierich A, et al. Disruption of the kappa-opioid receptor gene in mice enhances sensitivity to chemical visceral pain, impairs pharmacological actions of the selective kappa-agonist U-50,488H and attenuates morphine withdrawal. EMBO J. 1998;17:886–97.
7. Yaksh TL, Wallace MS. Opioids, analgesia, and pain management. In: Brunton LL, Chabner BA, Knollmann BC, editors. Goodman & Gilman's the pharmacological basis of therapeutics. 12th ed. McGraw-Hill Co., Inc; 2011.
8. Pande AC, Pyke RE, Greiner M, Wideman GL, Benjamin R, Pierce MW. Analgesic efficacy of enadoline versus placebo or morphine in postsurgical pain. Clin Neuropharmacol. 1996;19:451–6.
9. Kozono H, Yoshitani H, Nakano R. Post-marketing surveillance study of the safety and efficacy of nalfurafine hydrochloride (Remitch((R)) capsules 2.5 mug) in 3,762 hemodialysis patients with intractable pruritus. Int J Nephrol Renov Dis. 2018;11:9–24.
10. Kumagai H, Ebata T, Takamori K, Miyasato K, Muramatsu T, Nakamoto H, et al. Efficacy and safety of a novel k-agonist for managing intractable pruritus in dialysis patients. Am J Nephrol. 2012;36:175–83.
11. Kumagai H, Ebata T, Takamori K, Muramatsu T, Nakamoto H, Suzuki H. Effect of a novel kappa-receptor agonist, nalfurafine hydrochloride, on severe itch in 337 haemodialysis patients: a Phase III, randomized, double-blind, placebo-controlled study. Nephrol Dial Transplant. 2010;25:1251–7.
12. Nakao K, Mochizuki H. Nalfurafine hydrochloride: a new drug for the treatment of uremic pruritus in hemodialysis patients. Drugs Today. 2009;45:323–9.
13. von Voigtlander PF, Lahti RA, Ludens JH. U-50488: a selective and structurally novel non-Mu (kappa) opioid agonist. J Pharmacol Exp Ther. 1983;224:7–12.
14. Wang Y, Chen Y, Xu W, Lee DY, Ma Z, Rawls SM, et al. 2-Methoxymethyl-salvinorin B is a potent kappa opioid receptor agonist with longer lasting action in vivo than salvinorin A. J Pharmacol Exp Ther. 2008;324:1073–83.
15. Luttrell LM, Maudsley S, Bohn LM. Fulfilling the promise of "biased" G protein-coupled receptor agonism. Mol Pharmacol. 2015;88:579–88.
16. Rankovic Z, Brust TF, Bohn LM. Biased agonism: an emerging paradigm in GPCR drug discovery. Bioorg Med Chem Lett. 2016;26:241–50.
17. White KL, Robinson JE, Zhu H, DiBerto JF, Polepally PR, Zjawiony JK, et al. The G protein-biased kappa-opioid receptor agonist RB-64 Is analgesic with a unique spectrum of activities in vivo. J Pharmacol Exp Ther. 2015;352:98–109.
18. Ehrich JM, Messinger DI, Knakal CR, Kuhar JR, Schattauer SS, Bruchas MR, et al. Kappa opioid receptor-induced aversion requires p38 MAPK Aactivation in VTA dopamine neurons. J Neurosci. 2015;35:12917–31.
19. Bruchas MR, Land BB, Aita M, Xu M, Barot SK, Li S, et al. Stress-induced p38 mitogen-activated protein kinase activation mediates kappa-opioid-dependent dysphoria. J Neurosci. 2007;27:11614–23.

Phosphoproteomic approach for agonist-specific signaling in mouse brains:...
JJ Liu et al.

949

20. Bruchas MR, Macey TA, Lowe JD, Chavkin C. Kappa opioid receptor activation of p38 MAPK is GRK3- and arrestin-dependent in neurons and astrocytes. J Biol Chem. 2006;281:18081–9.

21. Bruchas MR, Schindler AG, Shankar H, Messinger DI, Miyatake M, Land BB, et al. Selective p38alpha MAPK deletion in serotonergic neurons produces stress resilience in models of depression and addiction. Neuron. 2011;71:498–511.

22. Zhou L, Bohn LM. Functional selectivity of GPCR signaling in animals. Curr Opin Cell Biol. 2014;27:102–8.

23. Aebersold R, Mann M. Mass-spectrometric exploration of proteome structure and function. Nature. 2016;537:347–55.

24. Humphrey SJ, Azimifar SB, Mann M. High-throughput phosphoproteomics reveals in vivo insulin signaling dynamics. Nat Biotechnol. 2015;33:990–5.

25. Riley NM, Coon JJ. Phosphoproteomics in the age of rapid and deep proteome profiling. Anal Chem. 2016;88:74–94.

26. Matthes HW, Maldonado R, Simonin F, Valverde O, Slowe S, Kitchen I, et al. Loss of morphine-induced analgesia, reward effect and withdrawal symptoms in mice lacking the mu-opioid-receptor gene. Nature. 1996;383:819–23.

27. Wang Y, Tang K, Inan S, Siebert D, Holzgrabe U, Lee DY, et al. Comparison of pharmacological activities of three distinct k ligands (Salvinorin A, TRK-820 and 3FLB) on k opioid receptors in vitro and their antipruritic and antinociceptive activities in vivo. J Pharmacol Exp Ther. 2005;312:220–30.

28. Murray CW, Porreca F, Cowan A. Methodological refinements to the mouse paw formalin test. An animal model of tonic pain. J Pharmacol Methods. 1988;20: 175–86.

29. Xu W, Wang Y, Ma Z, Chiu YT, Huang P, Rasakham K, et al. l-Isocorypalmine reduces behavioral sensitization and rewarding effects of cocaine in mice by acting on dopamine receptors. Drug Alcohol Depend. 2013;133:693–703.

30. Muschamp JW, Van't Veer A, Parsegian A, Gallo MS, Chen M, Neve RL, et al(2011). Activation of CREB in the nucleus accumbens shell produces anhedonia and resistance to extinction of fear in rats. J Neurosci. 31: 3095-103.

31. Cox J, Mann M. MaxQuant enables high peptide identification rates, individualized p.p.b.-range mass accuracies and proteome-wide protein quantification. Nat Biotechnol. 2008;26:1367–72.

32. Tyanova S, Temu T, Sinitcyn P, Carlson A, Hein MY, Geiger T, et al. The Perseus computational platform for comprehensive analysis of (prote)omics data. Nat Methods. 2016;13:731–40.

33. Cox J, Mann M. 1D and 2D annotation enrichment: a statistical method integrating quantitative proteomics with complementary high-throughput data. BMC Bioinform. 2012;13:S12.

34. Robles MS, Humphrey SJ, Mann M. Phosphorylation is a central mechanism for Circadian control of metabolism and physiology. Cell Metab. 2017;25:118–27.

35. Sacco F, Humphrey SJ, Cox J, Mischnik M, Schulte A, Klabunde T, et al. Glucose-regulated and drug-perturbed phosphoproteome reveals molecular mechanisms controlling insulin secretion. Nat Commun. 2016;7:13250.

36. Sharma K, Schmitt S, Bergner CG, Tyanova S, Kannaiyan N, Manrique-Hoyos N, et al. Cell type- and brain region-resolved mouse brain proteome. Nat Neurosci. 2015;18:1819–31.

37. Chen C, Chiu YT, Wu W, Huang P, Mann A, Schulz S, et al. Determination of sites of U50,488H-promoted phosphorylation of the mouse kappa opioid receptor (KOPR): disconnect between KOPR phosphorylation and internalization. Biochem J. 2016;473:497–508.

38. Seki T, Awamura S, Kimura C, Ide S, Sakano K, Minami M, et al. Pharmacological properties of TRK-820 on cloned mu-, delta- and kappa-opioid receptors and nociceptin receptor. Eur J Pharmacol. 1999;376:159–67.

39. Todtenkopf MS, Marcus JF, Portoghese PS, Carlezon WA Jr. Effects of kappa-opioid receptor ligands on intracranial self-stimulation in rats. Psychopharmacology. 2004;172:463–70.

40. Mansour A, Khachaturian H, Lewis ME, Akil H, Watson SJ. Anatomy of CNS opioid receptors. Trends Neurosci. 1988;11:308–14.

41. Geiger T, Wehner A, Schaab C, Cox J, Mann M. Comparative proteomic analysis of eleven common cell lines reveals ubiquitous but varying expression of most proteins. Mol Cell Proteom. 2012;11:M111 014050.

42. Amanchy R, Periaswamy B, Mathivanan S, Reddy R, Tattikota SG, Pandey A. A curated compendium of phosphorylation motifs. Nat Biotechnol. 2007;25:285–6.

43. Newman RH, Hu J, Rho HS, Xie Z, Woodard C, Neiswinger J, et al. Construction of human activity-based phosphorylation networks. Mol Syst Biol. 2013;9:655.

44. Harada H, Andersen JS, Mann M, Terada N, Korsmeyer SJ. p70S6 kinase signals cell survival as well as growth, inactivating the pro-apoptotic molecule BAD. Proc Natl Acad Sci USA. 2001;98:9666–70.

45. Morita T, Sobue K. Specification of neuronal polarity regulated by local translation of CRMP2 and Tau via the mTOR-p70S6K pathway. J Biol Chem. 2009;284:27734–45.

46. Biever A, Valjent E, Puighermanal E. Ribosomal protein S6 phosphorylation in the nervous system: from regulation to function. Front Mol Neurosci. 2015;8:75.

47. Jernigan CS, Goswami DB, Austin MC, Iyo AH, Chandran A, Stockmeier CA, et al. The mTOR signaling pathway in the prefrontal cortex is compromised in major depressive disorder. Prog Neuropsychopharmacol Biol Psychiatry. 2011;35: 1774–9.

48. Li N, Lee B, Liu RJ, Banasr M, Dwyer JM, Iwata M, et al. mTOR-dependent synapse formation underlies the rapid antidepressant effects of NMDA antagonists. Science. 2010;329:959–64.

49. Meikle L, Pollizzi K, Egnor A, Kramvis I, Lane H, Sahin M, et al. Response of a neuronal model of tuberous sclerosis to mammalian target of rapamycin (mTOR) inhibitors: effects on mTORC1 and Akt signaling lead to improved survival and function. J Neurosci. 2008;28:5422–32.

50. Blundell J, Kouser M, Powell CM. Systemic inhibition of mammalian target of rapamycin inhibits fear memory reconsolidation. Neurobiol Learn Mem. 2008;90:28–35.

51. Endoh T, Matsuura H, Tajima A, Izumimoto N, Tajima C, Suzuki T, et al. Potent antinociceptive effects of TRK-820, a novel kappa-opioid receptor agonist. Life Sci. 1999;65:1685–94.

52. Tsuji M, Takeda H, Matsumiya T, Nagase H, Narita M, Suzuki T. The novel kappa-opioid receptor agonist TRK-820 suppresses the rewarding and locomotor-enhancing effects of morphine in mice. Life Sci. 2001;68:1717–25.

53. Lazenka ML, Moerke MJ, Townsend EA, Freeman KB, Carroll FI, Negus SS (2018). Dissociable effects of the kappa opioid receptor agonist nalfurafine on pain/itch-stimulated and pain/itch-depressed behaviors in male rats. Psychopharmacology (Berl) 2018; 235: 203-213.

54. Ko MC, Husbands SM. Effects of atypical kappa-opioid receptor agonists on intrathecal morphine-induced itch and analgesia in primates. J Pharmacol Exp Ther. 2009;328:193–200.

55. Umeuchi H, Togashi Y, Honda T, Nakao K, Okano K, Tanaka T, et al. Involvement of central mu-opioid system in the scratching behavior in mice, and the suppression of it by the activation of kappa-opioid system. Eur J Pharmacol. 2003;477:29–35.

56. Endoh T, Tajima A, Suzuki T, Kamei J, Narita M, Tseng L, et al. Characterization of the antinociceptive effects of TRK-820 in the rat. Eur J Pharmacol. 2000;387:133–40.

57. Inan S, Dun NJ, Cowan A. Investigation of gastrin-releasing peptide as a mediator for 5′-guanidinonaltrindole-induced compulsive scratching in mice. Peptides. 2011;32:286–92.

58. Hoffert JD, Pisitkun T, Saeed F, Song JH, Chou CL, Knepper MA. Dynamics of the G protein-coupled vasopressin V2 receptor signaling network revealed by quantitative phosphoproteomics. Mol Cell Proteom. 2012;11:M111 014613.

59. Xiao K, Sun J, Kim J, Rajagopal S, Zhai B, Villen J, et al. Global phosphorylation analysis of beta-arrestin-mediated signaling downstream of a seven transmembrane receptor (7TMR). Proc Natl Acad Sci USA. 2010;107:15299–304.

60. Liu JJ, Sharma K, Zangrandi L, Chen C, Humphrey SJ, Chiu YT, et al. In vivo brain GPCR signaling elucidated by phosphoproteomics. Science. 2018;360. eaao4927 https://doi.org/10.1126/science.aao4927

61. Bailey J, Ma D, Szumlinski KK. Rapamycin attenuates the expression of cocaine-induced place preference and behavioral sensitization. Addict Biol. 2012;17:248–58.

62. Harraz MM, Tyagi R, Cortes P, Snyder SH. Antidepressant action of ketamine via mTOR is mediated by inhibition of nitrergic Rheb degradation. Mol Psychiatry. 2016;21:313–9.

63. Schattauer SS, Kuhar JR, Song A, Chavkin C. Nalfurafine is a G-protein biased agonist having significantly greater bias at the human than rodent form of the kappa opioid receptor. Cell Signal. 2017;32:59–65.

64. Morgenweck J, Frankowski KJ, Prisinzano TE, Aube J, Bohn LM. Investigation of the role of betaarrestin2 in kappa opioid receptor modulation in a mouse model of pruritus. Neuropharmacology. 2015;99:600–9.

65. Brust TF, Morgenweck J, Kim SA, Rose JH, Locke JL, Schmid CL, et al. Biased agonists of the kappa opioid receptor suppress pain and itch without causing sedation or dysphoria. Sci Signal. 2016;9:ra117.